http://www.pjbs.org

PJBS

ISSN 1028-8880

Pakistan Journal of Biological Sciences

ANSInet
Asian Network for Scientific Information
308 Lasani Town, Sargodha Road, Faisalabad - Pakistan

OPEN ACCESS Pakistan Journal of Biological Sciences

ISSN 1028-8880
DOI: 10.3923/pjbs.2025.735.748

Research Article
Diketopiperazines from the Endophytic *Streptomyces triticiradicis* TTCF1 (*Tinospora cordifolia*): Isolation and Evaluation of Antibacterial and Anticancer Properties

[1]Thongchai Taechowisan, [1]Janejira Wongpradit, [1]Thanaporn Chuen-Im and [2]Waya S. Phutdhawong

[1]Department of Microbiology, Faculty of Science, Silpakorn University, Nakhon Pathom 73000, Thailand
[2]Department of Chemistry, Faculty of Science, Silpakorn University, Nakhon Pathom 73000, Thailand

Abstract

Background and Objective: Endophytic actinomycetes associated with medicinal plants constitute a valuable yet underinvestigated source of bioactive secondary metabolites. *Tinospora cordifolia*, a widely respected ethnomedicinal plant, harbors diverse microbial endophytes with strong therapeutic potential. This study aimed to isolate and characterize endophytic actinomycetes from *T. cordifolia*, identify their major metabolites and evaluate the antibacterial, anticancer and molecular inhibitory properties of the purified compounds. **Materials and Methods:** Actinomycetes were isolated from surface-sterilized root, stem and leaf tissues using selective media. The most potent isolate, TTCF1, was identified through morphological characteristics, chemotaxonomic profiling and 16S rRNA gene sequencing. Bioactive metabolites were extracted and purified via column chromatography, followed by structural characterization using advanced spectroscopic techniques. Antibacterial activity was assessed by determining MIC and MBC values against human pathogens, including MRSA. Cytotoxicity was evaluated using the MTT assay on HeLa, HepG2 and MDA-MB-231 cancer cell lines, along with Vero cells as the non-cancerous control. Molecular docking was performed against EGFR, accompanied by ADMET property prediction. Statistical significance was determined using one-way ANOVA with Tukey's *post hoc* test ($p<0.05$). **Results:** Ten actinomycete isolates were obtained, all exclusively from root tissues. The strongest producer, TTCF1, showed 99.54% 16S rRNA similarity to *Streptomyces triticiradicis*. Chemical analysis yielded two diketopiperazines: Cyclo-(D-Pro-L-Tyr) and Cyclo-(D-Pro-L-Leu). Both compounds demonstrated potent antibacterial activity against Gram-positive pathogens (MIC 32-64 µg/mL) and cytotoxicity toward cancer cell lines (IC_{50} 58.16-362.71 µg/mL). Compound **1** showed selective toxicity toward HepG2 cells and exhibited stronger predicted EGFR binding affinity (-7.188 kcal/mol) than the reference inhibitor AQ4 (-6.703 kcal/mol). The ADMET profiles indicated good oral absorption. **Conclusion:** *Streptomyces triticiradicis* TTCF1 is a promising source of pharmacologically relevant diketopiperazines. Cyclo-(D-Pro-L-Tyr) emerges as a potential lead molecule with notable antimicrobial and selective anticancer activity, supported by strong EGFR-binding predictions.

Key words: Antibacterial activity, anticancer activity, diketopiperazines, endophyte, *Streptomyces triticiradicis* TTCF1

Citation: Taechowisan, T., J. Wongpradit, T. Chuen-Im and W.S. Phutdhawong, 2025. Diketopiperazines from the endophytic *Streptomyces triticiradicis* TTCF1 (*Tinospora cordifolia*): Isolation and evaluation of antibacterial and anticancer properties. Pak. J. Biol. Sci., 28: 735-748.

Corresponding Author: Thongchai Taechowisan, Department of Microbiology, Faculty of Science, Silpakorn University, 6 Rajamankanai Road, Nakhon Pathom 73000, Thailand

Competing Interest: The authors have declared that no competing interest exists.

Data Availability: All relevant data are within the paper and its supporting information files.

INTRODUCTION

Endophytes are microorganisms that inhabit the internal, healthy tissues of plants, establishing a symbiotic or mutualistic relationship with their host[1]. This unique biological niche offers a significant competitive advantage, as the microbes are protected from the intense competition present in the external soil environment[2].

Among these internal dwellers, endophytic actinomycetes, which are isolated following the surface-sterilization of plant tissues, have emerged as a particularly promising resource for discovering novel and potent bioactive natural compounds[3]. The theory underpinning this potential is that the long-term, intimate association of these microbes with the host plant, especially those with established medicinal value may drive the evolution of unique metabolic pathways. This is thought to result in the biosynthesis of chemically unique metabolites essential for their internal survival and interaction and potentially even the production of compounds structurally similar to the host plant's own natural products[4].

Tinospora cordifolia (family Menispermaceae) is a widely distributed climbing shrub highly valued in traditional medicine, particularly in Ayurveda, for its extensive therapeutic profile. This plant is native to several regions, including India, Bangladesh, Sri Lanka and Thailand and its genetic diversity underpins its common use in various local healing practices. Historically, the plant's roots, stem and leaves have been utilized to treat a broad spectrum of ailments, including fever, diabetes, jaundice, skin diseases, chronic diarrhea and rheumatism, often serving as a general rejuvenator and immunomodulatory agent. Furthermore, *T. cordifolia* is recognized for properties such as anti-inflammatory, anti-allergic, hepatoprotective and diuretic effects[5-7]. The plant's considerable medicinal activity is attributed to a rich profile of secondary metabolites, including compounds like tinosporine, tinosporide, cordifolide, cordifol, berberine and sitosterol[8,9].

Prior studies on *T. cordifolia* have confirmed the plant's capacity to host various endophytes that yield valuable natural products. Examples include a *Penicillium* species isolated from the plant that showed effective antibacterial action against *Bacillus subtilis* and *Staphylococcus aureus*[10]. Furthermore, the anticancer compound taxol was reported to be extracted from the endophytic fungus *Fusarium culmorum* residing within *T. cordifolia* tissues[11]. Other endophytic fungi from this host have been associated with anti-hyperuricemic (xanthine oxidase inhibition)[12], antimicrobial, antioxidant and antidiabetic activities[12-15].

Given the established traditional medicinal uses of *T. cordifolia* for numerous pathological conditions and the documented diverse biological activities of the host plant parts (including significant antimicrobial and cytotoxic effects), it is hypothesized that the associated endophytic microbes constitute a promising and untapped source of novel secondary metabolites[15]. While endophytic fungi from *T. cordifolia* have been relatively well-characterized, information concerning endophytic actinomycetes specifically from the *Tinospora* genus is notably limited.

Therefore, this study aims to explore the bioprospecting potential of these less-studied endophytic inhabitants. Specifically, the present investigation was undertaken to isolate and characterize endophytic actinomycetes from the leaf, stem and root tissues of *Tinospora cordifolia*. Subsequently, their extracts will be screened for significant antibacterial and anticancer (cytotoxic) properties, with the ultimate objective of isolating and identifying their major bioactive compounds.

MATERIALS AND METHODS

Study area: Experimental work was executed across the Departments of Microbiology and Chemistry at Silpakorn University, Nakhon Pathom, Thailand. The investigation period extended from April, 2024 to May, 2025.

Isolation of actinomycetes: Ten healthy specimens of *Tinospora cordifolia* (Willd.) Hook. f. and Thoms. were collected from Tambon Samphao Lom, Ayutthaya, Thailand (coordinates: 14.3421721 N, 100.5661420 E). Plant parts (leaves, stems and roots) were immediately separated and subjected to a rigorous surface sterilization protocol, adapted from the procedure of Taechowisan *et al.*[16] to eliminate external contaminants. Following sterilization, small segments of the plant tissues were cut and plated onto Humic Acid-Vitamins (HV) agar[17]. To selectively inhibit the growth of fungi and yeasts, the medium was supplemented with cycloheximide and nystatin (both at 100 µg/mL). Plates were incubated at 32°C for a period of three weeks. Colonies exhibiting the characteristic morphology of actinomycetes were selected and subsequently purified on International Streptomyces Project medium 2 (ISP-2) for long-term maintenance[18].

Antibacterial screening: Ten purified actinomycete isolates were initially screened for their ability to inhibit the growth of eight bacterial strains: *Bacillus cereus* TISTR687, *B. subtilis* TISTR008, *Escherichia coli* TISTR887, *Pseudomonas aeruginosa* TISTR1287, *Salmonella typhimurium* TISTR2519, *Staphylococcus aureus* TISTR885, *S. epidermidis* TISTR518 and a clinical isolate of methicillin-resistant *S. aureus* (MRSA) strain Sp3.

The antibacterial assay utilized a modified soft-agar overlay method[19]. All experiments were performed in triplicate and the resulting zones of inhibition were measured. The most potent isolate, designated TTCF1, was chosen for subsequent large-scale cultivation and advanced characterization.

Morphological and chemotaxonomic analysis: The selected potent isolate, TTCF1, was characterized using established morphological, physiological and chemotaxonomic techniques[20]. The detailed surface morphology of strain TTCF1 was visualized using Scanning Electron Microscopy (SEM), following a procedure adapted from Castillo *et al.*[21]. Samples were prepared, dried using a critical point dryer with liquid CO_2 (Quorum K850, UK) and sputter-coated with gold (Safematic CCU-010HV, Switzerland). The final observation was performed using a TESCAN Mira3 SEM (Czech Republic) to examine spore chains and surface ornamentation.

16S rDNA sequencing and phylogenetic analysis: Genomic DNA was extracted from TTCF1 cells harvested after seven days of cultivation in ISP-2 broth at 32°C with shaking (150 rpm) and subsequent washing with phosphate-buffered saline (PBS), using a commercial DNA extraction kit (Geneaid, Taiwan). The 16S ribosomal RNA gene (rDNA) was amplified via Polymerase Chain Reaction (PCR) using the universal primers A20F (5'-AGTTTGATCCTGGCTC3') and B1540R (5'-AAGGAGGTGATCCAGCC-3'). The resulting PCR product (approximately 1,500 bp) was purified using a commercial gel extraction kit (Geneaid, Taiwan) following agarose gel electrophoresis. Sequencing was conducted using the Sanger dideoxy chain termination method with the Big Dye Terminator cycle sequencing kit (Applied Biosystems, USA) on an automated sequencer (ABI PRISM 310 Genetic Analyzer, Applied Biosystems, USA). The assembled 16S rRNA sequence was deposited in the NCBI GenBank database and compared with known sequences using the Basic Local Alignment Search Tool (BLAST). Phylogenetic analysis was performed by aligning the TTCF1 sequence with reference sequences using CLUSTAL W (version 1.74) and constructing a phylogenetic tree based on the Neighbor-Joining method in MEGA 11 software[22].

Large-scale cultivation and crude extract preparation: The potent isolate TTCF1 was grown in bulk across 600 Petri dishes containing ISP-2 agar for 21 days at 32°C. The bacterial culture was then extracted using Ethyl Acetate (EtOAc) to recover the secondary metabolites[23]. The combined organic extracts were concentrated using a rotary evaporator, yielding a dark brown crude extract (~14.68 g). This crude extract was portioned: One part was dissolved in DMSO for biological testing and the remaining portion, solubilized in dichloromethane (CH_2Cl_2), was reserved for compound isolation.

Compound purification and characterization: A portion of the crude extract (~12.00 g) was separated using silica gel column chromatography with a gradient elution system of EtOAc in CH_2Cl_2. Fractions eluted with 25-30% EtOAc in CH_2Cl_2 were further purified via thin-layer chromatography (TLC) (mobile phase: EtOAc:CH_2Cl_2, 1:4), yielding compound **1** (~11.46 mg). Fractions eluted with 15-20% EtOAc in CH_2Cl_2 were similarly purified by TLC, resulting in compound **2** (~12.57 mg).

The chemical structures of the purified compounds were elucidated using various spectroscopic methods. Melting points were recorded. Ultraviolet (UV) absorption spectra, along with ^{1}H-NMR (300 MHz) and ^{13}C-NMR (100 MHz) spectra (Bruker Fourier 300 MHz spectrometer), provided detailed structural data. Mass spectrometry was used to confirm the molecular weights.

Determination of minimum inhibitory concentration (MIC) and minimum bactericidal concentration (MBC): The minimum inhibitory concentration (MIC) and minimum bactericidal concentration (MBC) for the crude extract and purified compounds were determined against the sensitive bacterial strains using established protocols described by Pfaller *et al.*[24], Chloramphenicol served as the positive control.

Cytotoxicity assay: The potential anticancer properties of the crude extract and purified compounds were evaluated using the standard MTT assay[25] against a panel of three human cancer cell lines: HeLa (cervical cancer), HepG2 (liver cancer) and MDA-MB-231 (breast cancer). A non-cancerous cell line, Vero, was included as a baseline control. Assays were conducted across a concentration range of 1-512 µg/mL. The selectivity index (SI) was calculated as the ratio of the IC_{50} (concentration inhibiting 50% growth) in Vero cells to the IC_{50} in each respective cancer cell line; a higher SI indicates greater selectivity. Doxorubicin hydrochloride was used as the positive control.

Molecular docking: The 3D structures of the ligands, Cyclo-(D-Pro-L-Tyr) and Cyclo-(D-Pro-L-Leu), were constructed and energy-minimized using UCSF Chimera software[26]. The target protein, Epidermal Growth Factor Receptor (EGFR) (PDB ID 1M17), was retrieved from the Protein Data Bank (www.rcsb.org). Molecular docking simulations were performed using AutoDock Vina within UCSF Chimera. A 25×25×25 A° cubic grid box was centered at the protein's active site, defined by the co-crystallized inhibitor ([6,7-bis(2-methoxy-ethoxy)quinazoline-4-yl]-(3-ethynylphenyl)amine: AQ4, DrugBank ID: DB00530). Results were reported as binding affinities (kcal/mol), with the lowest-energy conformation representing the optimal pose. Interactions (e.g., hydrogen bonds) were visualized using Discovery Studio Visualizer. Doxorubicin was the positive control.

ADMET prediction: *In silico* predictions of the Absorption, Distribution, Metabolism, Excretion and Toxicity (ADMET) properties for the ligands were conducted using the online tools SwissADME[27], Pre-ADMET[28] and pkCSM[29]. Doxorubicin and AQ4 were used as a reference compound for comparison.

Statistical analyses: All biological experiments were performed with three replicates. Data are expressed as the Mean±Standard Deviation (SD). Statistical analysis was conducted using SPSS for Windows, version 11.01 (SPSS Inc., Chicago, Illinois, USA). One-way Analysis of Variance (ANOVA), followed by Tukey's *post hoc* test, was used to determine statistically significant differences among groups. Differences were considered significant when the p-value <0.05.

RESULTS

The isolation process conducted on ten healthy *Tinospora cordifolia* specimens successfully yielded a total of 10 distinct actinomycete strains. Intriguingly, all ten isolates were recovered exclusively from the root segments of the host plant, with no successful isolation from stem or leaf tissues. All ten recovered isolates were subjected to an initial screening for antagonistic activity against a panel of human and plant pathogens. Among the isolates, strain TTCF1 demonstrated the most potent and promising bioactivity. Using the soft-agar overlay technique, TTCF1 showed significant inhibition zones, measuring between 32 mm and 45 mm against susceptible pathogens (Fig. 1). Based on this strong inhibitory performance, isolate TTCF1 was selected for detailed characterization and chemical investigation.

On ISP-2 agar, isolate TTCF1 exhibited characteristic actinomycete colony morphology, displaying a white spore mass over a leathery, cream-white substrate mycelium (Fig. 2a). After seven days of incubation, the initial white aerial mycelia matured, developing into an ash grey color. Microscopic examination, including Scanning Electron Microscopy (SEM), revealed that the aerial mycelia supported monopodially branched sporophores. The spores were flexible and oval in shape, presenting an immature smooth surface which transitioned to a distinctive spiny ornamentation upon maturation (Fig. 2b). The substrate and aerial mycelia were well-developed and did not exhibit fragmentation. Chemotaxonomic analysis further confirmed the presence of LL-diaminopimelic acid (LL-DAP) in the cell wall extract, definitively classifying the isolate within the genus *Streptomyces*.

Molecular identification was performed through 16S ribosomal RNA gene sequencing. Basic Local Alignment Search Tool (BLAST) analysis of the 16S rRNA sequence revealed that strain TTCF1 shared the highest sequence similarity (99.54%) with *Streptomyces triticiradicis* strain NEAU-H2. Other close genetic relatives included *S. rhizosphaerihabitans* (98.36%), *S. siamensis* (98.20%) and *S. populi* (98.16%). Phylogenetic analysis, conducted using the Neighbor-Joining method, provided further support for the identity, showing that isolate TTCF1 clustered strongly with the reference strain *S. triticiradicis* NEAU-H2 (Fig. 3). The partial 16S rRNA gene sequence for isolate TTCF1 was deposited in the GenBank database under the accession number PX468545.

A phylogenetic tree was constructed using the neighbor-joining method implemented in MEGA11 software. Bootstrap analysis (1000 replicates) was performed to assess the robustness of the tree topology, with bootstrap percentages displayed for each node (branch length representing 0.01 substitutions per site).

Large-scale fermentation of *S. triticiradicis* TTCF1 and subsequent solvent extraction yielded a dark brown crude extract. Chromatographic separation of this crude extract successfully led to the isolation and purification of two distinct secondary metabolites.

Compound 1: It was a white amorphous powder, MP 90°C-91°C, UV (MeOH)λ_{max}: 238 nm; ESI-MS m/z (rel. int.): 261.53 $[M+H]^+$, calcd. for $C_{14}H_{16}N_2O_3$, 260.28. ^{1}H-NMR ($CDCl_3$, δ, ppm, *J*/Hz): 12.04 (1H, s, 14-OH), 7.05 (2H, d, *J* = 8.5, H-12 and H-13), 6.82 (2H, d, *J* = 8.5, H-15 and H-16), 5.62 (1H, brs, NH), 4.21 (1H, m, H-3), 4.08 (1H, t, H-6), 3.61 (1H, m, H-3), 3.16 (1H, dd, *J* = 14.2 and 4.4, H-9), 2.76 (1H, dd, *J* = 6.1 and 2.1, H-10), 2.38 (1H, m, H-5), 2.03 (1H, m, H-10), 1.99 (1H, m, H-5), 1.88 (2H, m, H-4). ^{13}C-NMR ($CDCl_3$, δ, ppm, J/Hz): 169.9 (C-1), 165.4 (C-7), 132.6 (C-14), 130.7 (C-12), 129.1 (C-13), 128.3 (C-15), 127.4 (C-16), 58.8 (C-6), 56.3 (C-9), 45.5 (C-3), 40.7 (C-10), 35.9 (C-5), 24.4 (C-11) and 28.3 (C-4).

Fig. 1: Screening of antibacterial activity of *Streptomyces triticiradicis* TTCF1

Soft agar overlay technique was used to assess the antibacterial activity of a 7 days old preculture of *S. triticiradicis* TTCF1 (on ISP-2 medium) against the Methicillin-resistant *Staphylococcus aureus* (MRSA) Sp3. Inhibition zones were measured following 24 hrs of incubation at 37°C

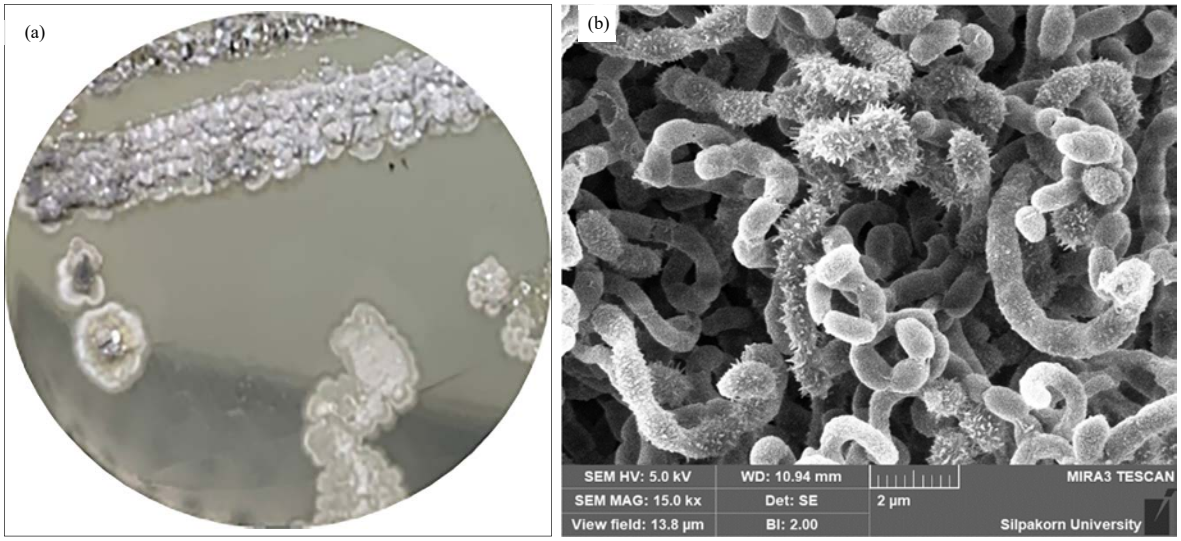

Fig. 2(a-b): Colony morphology and scanning electron micrograph of *Streptomyces triticiradicis* TTCF1, (a) Colony morphology of TTCF1 isolate grown on the ISP-2 agar after 15 days at 32°C incubation and (b) SEM micrograph of TTCF1, showing flexible spore chain, oval-shaped spores with immature smooth surface and mature spiny surface

Compound 2: It was a white amorphous powder, MP 160°C-162°C, UV (MeOH)λ_{max}: 210 nm; ESI-MS m/z (rel. int.): 211.12 $[M+H]^+$, calcd. for $C_{11}H_{18}N_2O_2$, 210.27. ^{1}H-NMR ($CDCl_3$, δ, ppm, *J*/Hz): 6.38 (1H, brs, NH), 4.54 (1H, dt, *J* = 8.2 and 1.1, H-6), 4.10 (1H, dd, *J* = 9.2 and 4.4, H-9), 3.54 -3.70 (2H, m, H-3), 2.31 (1H, m, H-5), 2.15 (1H, m, H-4), 2.10 (1H, m, H-4), 2.02 (1H, m, H-4), 1.92 (1H, m, H-10), 1.86 (1H, m, H-10), 1.55 (1H, m, *J* = 4.9, 9.3 and 14.2, H-11), 0.98 (3H, d, *J* = 6.4, CH_3), 0.95 (3H, d, *J* = 6.5, CH_3). ^{13}C-NMR ($CDCl_3$, δ, ppm, J/Hz): 170.3 (C-1), 166.4 (C-7), 59.2 (C-6), 53.5 (C-9), 45.4 (C-3), 38.4 (C-10), 28.2 (C-5) 24.6 (C-11), 23.2 (C-4), 22.7 (C-12) and 21.3 (C-13).

Spectroscopic analyses (UV, ^{1}H-NMR, ^{13}C-NMR and Mass Spectrometry) confirmed the compounds' structures, identifying compound **1** as Cyclo-(D-Pro-L-Tyr) and compound **2** as Cyclo-(D-Pro-L-Leu). Both compounds belong to the diketopiperazine class. The molecular structures of compounds **1** and **2** are presented in Fig. 4. The final yields corresponded to 1.17 mg/L of culture medium for compound **1** and 1.28 mg/L of culture medium for compound **2**.

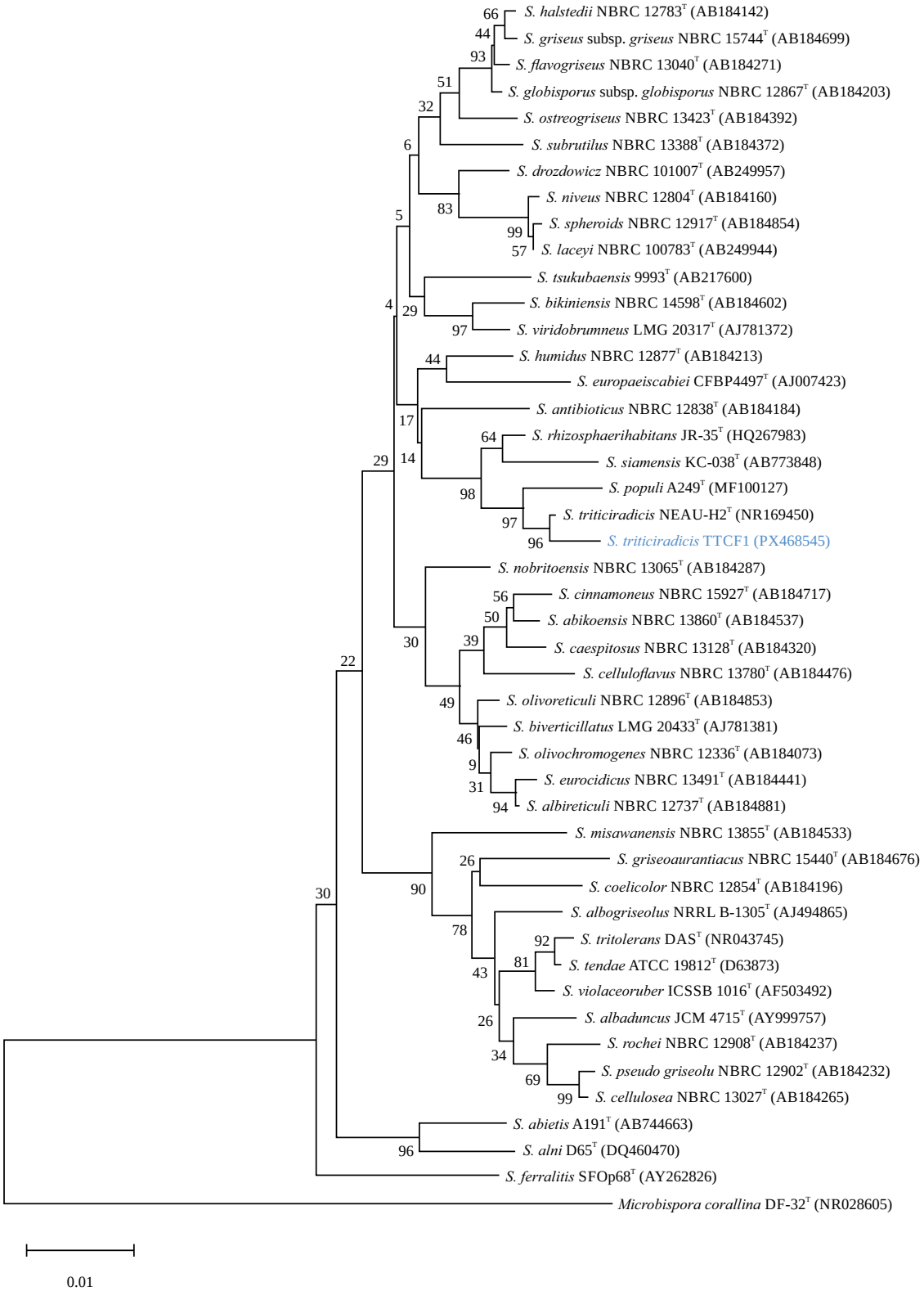

Fig. 3: Phylogenetic analysis of 16SrDNA gene sequences of *Streptomyces triticiradicis* TTCF1 and related type strains were retrieved from GenBank (accession numbers in parentheses)

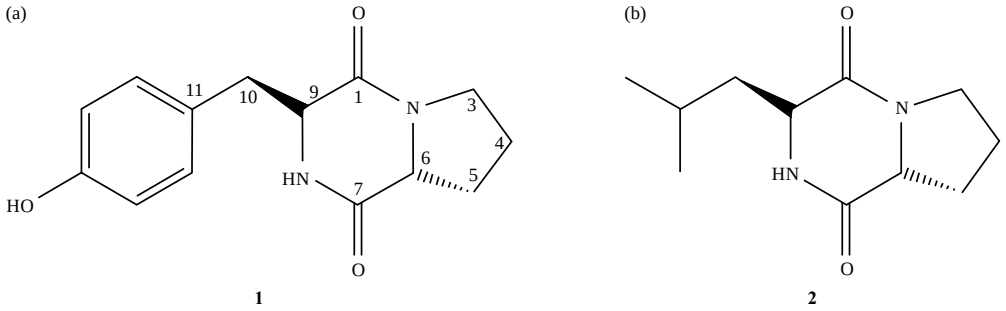

Fig. 4(a-b): Structures of the compounds, (a) Cyclo-(D-Pro-L-Tyr) (**1**) and (b) Cyclo-(D-Pro-L-Leu) (**2**)

Table 1: MIC and MBC of the purified compounds and chloramphenicol against tested bacteria

	MIC (µg/mL)			MBC (µg/mL)		
Test organisms	Compound **1**	Compound **2**	Chloramphenicol	Compound **1**	Compound **2**	Chloramphenicol
S. aureus TISTR885	32	32	2	128	128	16
S. epidermidis TISTR518	32	32	2	128	128	16
B. cereus TISTR687	64	64	2	256	256	16
B. subtilis TISTR008	64	64	2	256	256	16
E. coli TISTR887	256	256	16	>512	>512	64
S. typhimurium TISTR292	256	256	16	>512	>512	64
P. aeruginosa TISTR1287	512	512	32	>512	>512	128
MRSA Sp3*	32	64	16	128	256	128

*Clinical isolate: Methicillin-resistant *S. aureus* strain Sp3

Table 2: IC_{50} values and selectivity indices (SI) of crude extract and purified compounds against cancer cell lines

	Vero cells	MDA-MB-231 cells		HeLa cells		HepG2 cells	
Test substances	IC_{50} (µg/mL)	IC_{50} (µg/mL)	SI	IC_{50} (µg/mL)	SI	IC_{50} (µg/mL)	SI
Crude extract	577.86±82.69[a]	424.07±42.33[a]	1.36	465.20±53.72[a]	1.24	556.48±87.04[a]	1.04
Compound **1**	386.45±57.02[b]	58.16±12.47[b]	6.64	97.38±27.44[b]	3.97	207.85±67.18[b,c]	1.86
Compound **2**	403.67±65.73[b]	67.90±18.25[b]	5.95	122.50±30.26[b]	3.30	362.71±72.29[b]	1.11
Doxorubicin hydrochloride	124.30±17.62[c]	8.17±4.55[b]	15.21	7.43±4.65[c]	16.73	120.74±28.36[c]	1.03

Vero cells: African green monkey kidney cell line, MDA-MB-231 cells: Human breast cancer cell line, HeLa cells: Human cervical carcinoma cell line, HepG2: Human hepatocellular carcinoma cell line. IC_{50} values represent the concentration causing 50% growth inhibition. The values are expressed as Mean±Standard Deviation of the three replicates. SI: Selectivity indices (SI) were calculated as the ratio of the IC_{50} in the Vero cell line to the IC_{50} in the cancer cell lines. [a,b,c]Different letters indicated statistically significant differences within the same category ($p<0.05$)

The two purified diketopiperazine compounds exhibited moderate to good antibacterial activity (Table 1). The antibacterial efficacy was notably higher against Gram-positive bacteria, including the clinical Methicillin-resistant *S. aureus* MRSA) strain Sp3. For Gram-positive pathogens, the minimum inhibitory concentration (MIC) values ranged from 32 to 64 µg/mL and the minimum bactericidal concentration (MBC) values ranged from 128 to 256 µg/mL. Conversely, the compounds displayed lower potency against Gram-negative bacteria, with MIC values falling between 256 and 512 µg/mL and MBC values exceeding 512 µg/mL.

The cytotoxicity of the crude extract and the purified compounds was assessed against three human cancer cell lines HeLa, HepG2 and MDA-MB-231) and a non-cancerous control cell line (Vero). The compounds showed significant cytotoxic effects on the cancer cell lines, with IC_{50} values ranging from 58.16 to 362.71 µg/mL. Critically, the crude extract and purified compounds demonstrated only moderate cytotoxicity against the non-cancerous Vero cells IC_{50} values ranging from 386.45 to 577.86 µg/mL). The selectivity index (Table 2), which measures the preference for cancer cells over normal cells, was calculated. Against the HepG2 (liver cancer) cell line, the SI for the extract and purified compounds was higher than that of the positive control, doxorubicin hydrochloride. This suggests a more selective cytotoxic effect toward this specific liver cancer line. In contrast, the SI values for the MDA-MB-231 and HeLa cell lines were lower than those of doxorubicin.

These collective findings indicate that the root tissues of *T. cordifolia* are a valuable ecological source for isolating actinomycetes, such as *S. triticiradicis* TTCF1, capable of producing active compounds with significant antibacterial and selective anticancer potential.

Table 3: Results of predictions of molecular interaction between the EGFR protein and the test compounds

Purified compounds	Binding energy (kcal/mol)	Interaction types	Hydrogen bonds		Bond length (A°)	Docking site
			H-bond donors	H-bond acceptors		
Compound **1**	-7.188	CoH	Met769: HN	LIG: O	2.17560	Active pocket site
		CoH	LIG: H	Pro770: O	2.15406	
		CoH	LIG: H	Met769: O	2.81795	
		A	Val702 (Alkyl)	LIG: (Alkyl)	4.85406	
		A	Ala719 (Alkyl)	LIG: (Alkyl)	4.63029	
		A	LIG: (Alkyl)	Leu820 (Alkyl)	4.97364	
		Pi-A	LIG: (Pi-orbitals)	Leu694 (Alkyl)	4.02697	
Compound **2**	-5.634	CoH	Asp831: HN	LIG: O	2.53868	Active pocket site
		CoH	LIG: H	Asp831: OD2	2.54845	
		A	Ala719 (Alkyl)	LIG: C (Alkyl)	3.82141	
		A	Lys721 (Alkyl)	LIG: (Alkyl)	4.07885	
		A	LIG: (Alkyl)	Leu820 (Alkyl)	4.46564	
		A	LIG: (Alkyl)	Met742 (Alkyl)	5.18127	
		A	LIG: (Alkyl)	Leu764 (Alkyl)	4.24433	
Doxorubicin	-9.779	CoH	Met769: HN	LIG: O	2.94772	Active pocket site
		CoH	LIG: H	Arg817: O	2.68598	
		CoH	LIG: H	Asn818: OD1	1.98504	
		CoH	LIG: H	Arg817: O	2.56187	
		CaH	Asp831: HA	LIG: O	2.69827	
		AC	LIG: N (Positive)	Asp831: OD2 (Negative)	4.37514	
		Pi-S	Val702: HG13 (C-H)	LIG: (Pi-orbitals)	2.49538	
		Pi-S	LIG: C (C-H)	Phe699 (Pi-orbitals)	3.57587	
		Pi-A	LIG: (Pi-orbitals)	Leu694 (Alkyl)	5.32423	
		Pi-A	LIG: (Pi-orbitals)	Ala719 (Alkyl)	5.16600	
		Pi-A	LIG: (Pi-orbitals)	Leu820 (Alkyl)	5.17351	
		Pi-A	LIG: (Pi-orbitals)	Leu694 (Alkyl)	3.89900	
		Pi-A	LIG: (Pi-orbitals)	Leu694 (Alkyl)	3.85830	
AQ4	-6.703	CoH	Met769: HN	LIG: O	2.10135	Active pocket site
		CoH	LIG: H	Arg817: O	2.10922	
		CaH	Leu768: HA	LIG: O	2.90514	
		CaH	LIG: C	Met769: O	3.59599	
		Pi-A	Phe699 (Pi-orbitals)	LIG: C (Alkyl)	3.61046	
		Pi-A	LIG: (Pi-orbitals)	Val702 (Alkyl)	5.01006	
		Pi-A	LIG: (Pi-orbitals)	Leu820 (Alkyl)	4.66201	
		Pi-A	LIG: (Pi-orbitals)	Cys773 (Alkyl)	4.32075	
		Pi-A	LIG: (Pi-orbitals)	Arg817 (Alkyl)	4.97862	

EGFR protein; PDB ID: 1M17. Interaction types; CoH: Conventional hydrogen bond, CaH: Carbon hydrogen bond, AC: Attractive charge interaction, A: Alkyl interaction, Pi-A: Pi-Alkyl interaction and Pi-S: Pi-Sigma interaction. LIG; Ligand: Compounds **1**, **2**, ([6,7-bis(2-methoxy-ethoxy)quinazoline-4-yl]-(3-ethynylphenyl)amine (AQ4) and doxorubicin

Molecular docking simulations were executed to investigate the potential mechanism of action for the isolated compounds **1** and **2**, by assessing their binding affinity for the Epidermal Growth Factor Receptor (EGFR) (PDB ID: 1M17). The known inhibitor AQ4 and the positive control doxorubicin were used as reference ligands. All four molecules successfully demonstrated favorable binding within the active site of the EGFR structure.

The calculated binding energies (Table 3) showed a range of affinities. Doxorubicin exhibited the strongest predicted binding (-9.779 kcal/mol), followed by compound **1** (-7.188 kcal/mol), AQ4 (-6.703 kcal/mol) and compound **2** (-5.634 kcal/mol). A significant finding was that the predicted binding affinity of compound **1** (-7.188 kcal/mol) surpassed that of the reference small-molecule inhibitor AQ4 (-6.703 kcal/mol), suggesting a more stable theoretical interaction with the target protein. Hydrogen bonding was identified as the primary stabilizing interaction for the ligand-protein complexes. The compounds exhibited distinct binding patterns: Compound **1** formed hydrogen bonds with the amino acid residues Met769 and Pro770 (Fig. 5a-b). compound **2** formed a hydrogen bond with Asp831 (Fig. 5c-d). Doxorubicin was observed to form hydrogen bonds with key amino acid residues, including Met769, Arg817, Asn818 and Asp831 (Fig. 5e-f). In contrast, AQ4 formed hydrogen bonds primarily with Leu768, Met769 and Arg817 (Fig. 5g-h). This analysis confirms that both isolated diketopiperazines can successfully interact with the EGFR active site like doxorubicin and its small molecule inhibitor, providing initial computational support for their observed cytotoxicity. Detailed information, including the specific hydrogen bond interactions, bond lengths and amino acid residues involved in binding, is presented in Table 3.

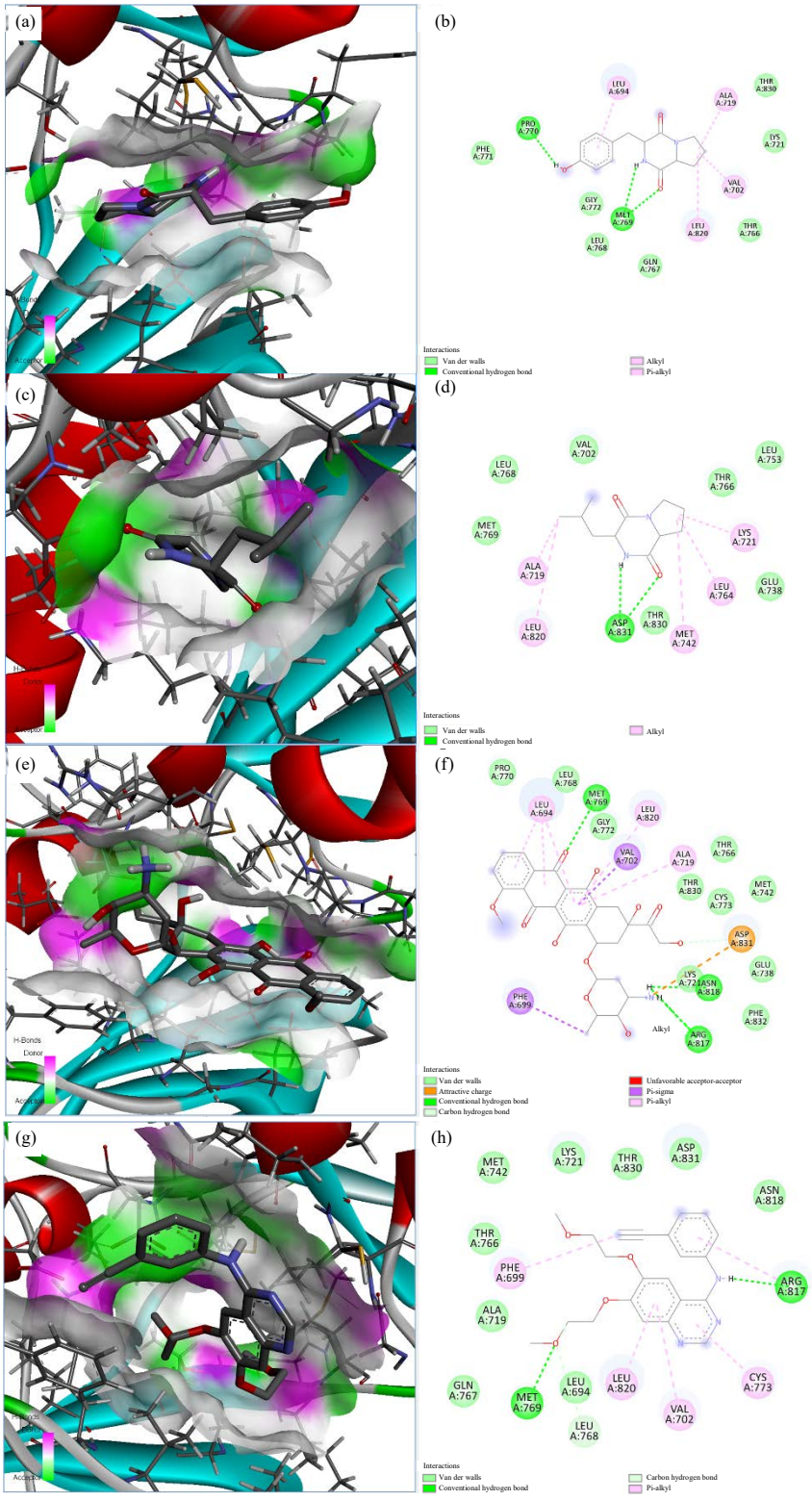

Fig. 5(a-h): Crystal structure interaction and Two-dimensional (2D) illustration between the compound agents and the active sites of the EGFR; (a-b) Compound **1**, (c-d) Compound **2**, (e-f) Doxorubicin and (g-h) [6,7-bis(2-methoxy-ethoxy)quinazoline-4-yl]-(3-ethynylphenyl)amine: AQ4

Hydrogen bond donors and acceptors are represented around the binding cavity in pink and green, respectively. Dark green, light green, pale purple, pale pink, short pale pink and long brown dashes represent conventional hydrogen bonds, carbon hydrogen bonds as well as pi-sigma, alkyl, pi-alkyl bonds and attractive charge interactions, respectively. Amino acids in pale green exhibit Van der Waals interactions

Table 4: Predicted absorption, distribution, metabolism, excretion and toxicity properties of the compound agents

	Compound agents			
Properties[a]	Compound **1**	Compound **2**	AQ4[b]	Doxorubicin
TPSA	69.64	49.41	74.73	206.07
Consensus log $P_{o/w}$	0.84	0.96	3.23	0.52
Absorption				
Water solubility (log S)	−2.08	−1.75	−4.56	−5.20
Caco2 cell permeability	21.82	21.38	54.88	17.72
Human intestinal absorption (absorbed (%))	77.38	84.72	97.28	62.13
Skin permeability (log Kp cm/sec)	−3.511	−3.763	−2.984	−2.735
P-Glycoprotein substrate	Yes	Yes	Yes	Yes
P-Glycoprotein inhibitor	No	No	Yes	No
Distribution				
BBB permeability (log BBB)	0.5357	0.4325	0.0416	0.0328
Metabolism				
CYP2D6 substrate	No	No	No	No
CYP3A4 substrate		No	Yes	No
CYP1A2 inhibitor	No	No	No	No
CYP2C19 inhibitor	No	No	Yes	No
CYP2C9 inhibitor	No	No	Yes	No
CYP2D6 inhibitor	No	No	No	No
CYP3A4 inhibitor	No	No	No	No
Excretion				
Renal OCT2 substrate	No	No	No	No
Toxicity				
Ames_test	Mutagen	Mutagen	Mutagen	Mutagen
Carcino_mouse	No	No	No	No
Carcino_rat	No	Yes	No	No
TA100_10RLI	No	Yes	Yes	No
TA100_NA	No	No	No	No
TA1535_10RLI	No	Yes	No	No
TA1535_NA	No	No	No	No
hERG inhibitor	Low risk	Low risk	Medium risk	Medium risk
Hepatotoxicity	No	No	Yes	Yes
Skin sensitization	No	No	No	No

[a]BBB: Blood-brain barrier, CYP: Cytochrome p450, Caco2: Caucasian colon adenocarcinoma cell line, hERG: Human ether-a-go-go-related gene, Kp: Skin permeability constant, log $P_{o/w}$: Log of relative solubility of the drug in n-octanol, OCT2: Organic cation transporter 2, TPSA: Topological polar surface area and [b]AQ4: [6,7-bis(2-methoxy-ethoxy)quinazoline-4-yl]-(3-ethynylphenyl)amine

The pharmacokinetic profile of compounds **1** and **2** was virtually screened using ADMET prediction tools (SwissADME, Pre-ADMET and pkCSM) and compared against AQ4 and doxorubicin (Table 4). Absorption: Both compound **1** (77.38%) and compound **2** (84.72%) showed a high predicted human intestinal absorption (HIA). This HIA was significantly better than the predicted value for doxorubicin (62.13%) but lower than that of AQ4 (97.28%). Additionally, both compounds were predicted to exhibit high Caco-2 permeability. Both compounds were predicted to be P-glycoprotein (P-gp) substrates, which may limit their oral bioavailability, though they were not predicted to be P-gp inhibitors.

Distribution and metabolism: Both compounds showed high predicted Blood-Brain Barrier penetration (BBB>0.3). They were not predicted to act as substrates or inhibitors for any tested CYP450 isoforms.

Toxicity: The toxicity predictions indicated areas for caution. Compound **2** specifically flagged potential mutagenicity in the Ames test (TA100_10RLI and TA1535_10RLI strains) and potential carcinogenicity in rats (though not in mice). Conversely, a low risk of hERG channel inhibition (cardiotoxicity) was predicted for both compounds.

DISCUSSION

The current investigation successfully isolated and characterized the endophytic actinomycete *Streptomyces triticiradicis* TTCF1 from the root tissue of *Tinospora cordifolia*. Furthermore, this microbe was found to be a producer of two known diketopiperazine (DKP) derivatives: Cyclo-(D-Pro-L-Tyr) (compound **1**) and Cyclo-(D-Pro-L-Leu) (compound **2**). The structural assignments were fully verified by comparing the spectroscopic data of the purified compounds with previously published reports. It is noteworthy that these specific DKPs

have also been isolated from diverse microbial sources, including *Bacillus* species[30] and other bacteria associated with invertebrates[31]. The isolation of *S. triticiradicis* TTCF1 from *T. cordifolia* roots further supports the recognition of plant endophytes as a vital reservoir for novel and active secondary metabolites[32,33].

The production efficiency under non-optimized culture conditions was favorable, yielding 1.17 mg/L for compound **1** and 1.28 mg/L for compound **2**. These yields are competitive with or superior to those reported in the literature for similar DKPs from other bacterial species. For instance, the yield of compound **2** (1.28 mg/L) significantly surpasses the 0.19 mg/L yield of Cyclo(L-Pro-L-Leu) reported from *Lysobacter capsici*[34]. While DKP production in *Streptomyces* species shows high variability[35-37], the yields achieved here suggest that *S. triticiradicis* TTCF1 is an efficient producer, highlighting the potential for enhanced yields through the optimization of fermentation parameters. Phylogenetic analysis indicated that strain TTCF1 is highly similar to *S. triticiradicis* NEAU-H2, which was previously isolated from wheat rhizosphere soil[38].

The isolated DKPs primarily exhibited strong antimicrobial activity against Gram-positive bacteria, including the clinically relevant MRSA strain, with MIC values ranging from 32 to 64 µg/mL. Conversely, the compounds showed low activity against Gram-negative bacteria. This pattern is consistent with previous findings for these specific DKP structures[39,40]. Literature reports confirm that other diketopiperazines, such as Cyclo-(L-Pro-L-Val), show potent activity against Gram-positive bacteria within a similar MIC range (32 to 256 µg/mL)[37]. The observed selectivity suggests that the mechanism of action may target unique features of the Gram-positive cell wall, warranting further investigation.

The DKPs are a well-documented class of metabolites with diverse biological actions, including cytotoxicity and apoptosis induction in cancer cells[41,42]. The current results demonstrated potent cytotoxic effects for the isolated DKPs against all tested cancer cell lines (MDA-MB-231, HeLa and HepG2), with IC_{50} values ranging from 58.16 to 362.71 µg/mL. These values underscore their potential as promising anticancer agents.

However, the moderate cytotoxicity observed against the non-cancerous Vero cell line (IC_{50} values ranging from 386.45 to 403.67 µg/mL) highlights a critical need for enhancing selectivity. While the selectivity index against the HepG2 cell line was favorable compared to doxorubicin, minimizing off-target toxicity to healthy cells is a necessary consideration for therapeutic development[43].

To explore a plausible mechanism for the observed anticancer effect, molecular docking was performed against the Epidermal Growth Factor Receptor (EGFR) (PDB ID: 1M17), a receptor tyrosine kinase commonly overexpressed in various cancers[44]. This approach is supported by previous studies utilizing cyclic dipeptide structures for the design of novel EGFR kinase inhibitors[45]. Both isolated DKPs exhibited favorable predicted binding energies. Crucially, compound **1** (-7.188 kcal/mol) displayed a stronger binding affinity than the reference small-molecule inhibitor AQ4 (-6.703 kcal/mol). This lower binding energy suggests a more stable interaction and exceptional potential for compound **1** as an EGFR inhibitor. The docking analysis revealed that the L-Tyr moiety of compound **1** is key to its interaction, forming a critical hydrogen bond with the Pro770 residue of EGFR. Furthermore, compound **1** showed binding patterns and interactions (e.g., hydrogen bond with Met769) similar to the positive control, doxorubicin, suggesting a comparable inhibitory mechanism within the EGFR active site.

The ADMET predictions are vital for screening drug candidates[46]. The virtual screen indicated that both DKPs possess favorable oral absorption characteristics.

Absorption: Both compounds **1** (77.38%) and 2 (84.72%) had high predicted Human Intestinal Absorption (HIA), a significant advantage over doxorubicin (62.13%)[47]. They also showed high predicted Caco-2 permeability[48]. However, their prediction as P-glycoprotein (P-gp) substrates could potentially reduce oral bioavailability, though the lack of P-gp inhibition suggests a lower risk of adverse drug-drug interactions[48].

Metabolism/excretion: The compounds were not predicted to interact with any tested CYP450 isoforms.

Toxicity: The toxicity profile necessitates caution. Compound **2** was flagged for potential mutagenicity in specific Ames test strains and predicted carcinogenicity in rats[49]. Furthermore, while the risk was low, hERG channel inhibition was predicted, which is an important consideration for potential cardiotoxicity[47]. These preliminary toxicity flags highlight the need for extensive *in vitro* and *in vivo* toxicological studies during future compound optimization.

In summary, the root tissue of *T. cordifolia* proved to be a valuable niche for isolating *S. triticiradicis* TTCF1, a source of biologically active diketopiperazines with promising antimicrobial and selective anticancer potential.

CONCLUSION

The root-associated endophyte *S. triticiradicis* TTCF1 represents an efficient natural source for bioactive diketopiperazines: Cyclo-(D-Pro-L-Tyr) (compound **1**) and Cyclo-(D-Pro-L-Leu) (compound **2**). They exhibited strong antimicrobial efficacy against Gram-positive pathogens, including a clinical MRSA strain and potent cytotoxicity against various human cancer cell lines (HeLa, HepG2 and MDA-MB-231). Molecular docking simulations provided mechanistic insight, revealing that compound **1** possesses a particularly favorable binding affinity for the EGFR active site, surpassing that of the reference small-molecule inhibitor AQ4. While potential toxicity concerns, particularly mutagenicity flagged for compound **2**, necessitate caution, these findings strongly validate the need for continued bioprospecting of endophytes from *T. cordifolia*. Future work should focus on optimizing the fermentation yield, conducting targeted *in vitro* EGFR inhibition assays and performing comprehensive *in vivo* efficacy and toxicological studies to advance compound **1** toward preclinical development.

SIGNIFICANCE STATEMENT

This research establishes the root endophyte *Streptomyces triticiradicis* TTCF1 isolated from the highly medicinal *Tinospora cordifolia* as a novel and efficient source of bioactive diketopiperazines. Facing the urgent global need for new drug leads against infectious diseases and cancer, this study identifies Cyclo-(D-Pro-L-Tyr) (compound **1**) as a highly promising candidate. Compound **1** exhibits potent activity against the drug-resistant pathogen MRSA and various cancer cell lines. Crucially, molecular docking analysis reveals that compound 1 has a superior predicted binding affinity to the Epidermal Growth Factor Receptor (EGFR), a common cancer target compared to a commercial reference inhibitor. This finding positions *S. triticiradicis* TTCF1 as a valuable bioprospecting strain and compound **1** as a prime preclinical lead for developing dual-action therapeutic agents.

ACKNOWLEDGMENT

This work was supported by a research grant (No. SRIF-JRG-2568-08) from the Faculty of Science, Silpakorn University, Nakhon Pathom, Thailand.

REFERENCES

1. Khare, E., J. Mishra and N.K. Arora, 2018. Multifaceted interactions between endophytes and plant: Developments and prospects. Front. Microbiol., Vol. 9. 10.3389/fmicb.2018.02732.
2. Chaudhary, P., U. Agri, A. Chaudhary, A. Kumar and G. Kumar, 2022. Endophytes and their potential in biotic stress management and crop production. Front. Microbiol., Vol. 13. 10.3389/fmicb.2022.933017.
3. Matsumoto, A. and Y. Takahashi, 2017. Endophytic actinomycetes: Promising source of novel bioactive compounds. J. Antibiot., 70: 514-519.
4. Kandasamy, G.D. and P. Kathirvel, 2023. Insights into bacterial endophytic diversity and isolation with a focus on their potential applications-A review. Microbiol. Res., Vol. 266. 10.1016/j.micres.2022.127256.
5. Balkrishna, A., A. Kumar, A. Rohela, V. Arya and A.K. Gautam *et al*., 2024. Traditional uses, hepatoprotective potential, and phytopharmacology of *Tinospora cordifolia*: A narrative review. J. Pharm. Pharmacol., 76: 183-200.
6. Sharma, A., P. Bajaj, A. Bhandari and G. Kaur, 2020. From ayurvedic folk medicine to preclinical neurotherapeutic role of a miraculous herb, *Tinospora cordifolia*. Neurochem. Int., Vol. 141. 10.1016/j.neuint.2020.104891.
7. Ahsan, R., A. Mishra, B. Badar, M. Owais and V. Mishra, 2023. Therapeutic application, phytoactives and pharmacology of *Tinospora cordifolia*: An evocative review. Chin. J. Integr. Med., 29: 549-555.
8. Kumar, P., M. Kamle, D.K. Mahato, H. Bora, B. Sharma, P. Rasane and V.K. Bajpai, 2020. *Tinospora cordifolia* (Giloy): Phytochemistry, ethnopharmacology, clinical application and conservation strategies. Curr. Pharm. Biotechnol., 21: 1165-1175.
9. Chi, S., G. She, D. Han, W. Wang, Z. Liu and B. Liu, 2016. Genus *Tinospora*: Ethnopharmacology, phytochemistry, and pharmacology. Evidence-Based Complementary Altern. Med., Vol. 2016. 10.1155/2016/9232593.
10. Desai, S., R. Metrani, S. Vantamuri, V. Ginigeri, K. Phadke and B. Hungund, 2012. Phytochemical analysis, antimicrobial and antitumour screening of endophytes of *Tinospora cordifolia*. Int. J. Pharma Biosci., 3: 533-540.
11. Sonaimuthu, V., S. Krishnamoorthy and M. Johnpaul, 2010. Taxol producing endophytic fungus *Fusarium culmorum* SVJM072 from medicinal plant of *Tinospora cordifolia*-a first report. J. Biotechnol., 150: 425-425.
12. Kapoor, N. and S. Saxena, 2018. Endophytic fungi of *Tinospora cordifolia* with anti-gout properties. 3 Biotech, Vol. 8. 10.1007/s13205-018-1290-3.

13. Habbu, P.V., S.D. Madagundi and V.H. Kulkarni, 2021. Antioxidant and antidiabetic potential of endophytic fungal fractions recovered from *Tinospora cordifolia* (Willd.) leaves. RGUHS J. Pharm. Sci., Vol. 11. 10.26463/rjps.11_2_2.
14. Singh, B. and P. Kumar, 2020. Antiphytopathogenic potential of phenolic compounds of endophytic *Cladosporium velox* isolated from *Tinospora cordifolia*. Org. Med. Chem. Int. J., Vol. 10. 10.19080/OMCIJ.2020.10.555787.
15. Murshid, G.M., M.H. Sohrab, K.S. Ahmed, M.M. Masud and M. Abdul Mazid, 2022. Antiproliferative and antibacterial potentials of endophytic fungi associated with Bangladeshi medicinal plant *Tinospora cordifolia*. Dhaka Univ. J. Pharm. Sci., 21: 183-194.
16. Taechowisa, T., T. Chuen-Im and W.S. Phutdhawon, 2025. Antibacterial and anticancer properties of anthraquinones from *Streptomyces galbus* AVL08, an endophyte in *Aloe vera* Linn. Pak. J. Biol. Sci., 28: 344-358.
17. Otoguro, M., M. Hayakawa, T. Yamazaki and Y. Iimura, 2001. An integrated method for the enrichment and selective isolation of *Actinokineospora* spp. in soil and plant litter. J. Appl. Microbiol., 91: 118-130.
18. Shirling, E.B. and D. Gottlieb, 1966. Methods for characterization of *Streptomyces* species. Int. J. Syst. Bacteriol., 16: 313-340.
19. Hockett, K.L. and D.A. Baltrus, 2017. Use of the soft-agar overlay technique to screen for bacterially produced inhibitory compounds. J. Visualized Exp., Vol. 119. 10.3791/55064.
20. Cassarini, M., C. Rémond, E. Mühle, D. Clermont and L. Besaury, 2022. *Streptomyces durocortorensis* sp. nov., isolated from oak rhizosphere. Int. J. Syst. Evol. Microbiol., Vol. 72. 10.1099/ijsem.0.005480.
21. Castillo, U.F., G.A. Strobel, E.J. Ford, W.M. Hess and H. Porter *et al*., 2002. Munumbicins, wide-spectrum antibiotics produced by *Streptomyces* NRRL 30562, endophytic on *Kennedia nigriscans*. Microbiology, 148: 2675-2685.
22. Tamura, K., G. Stecher and S. Kumar, 2021. MEGA11: Molecular evolutionary genetics analysis version 11. Mol. Biol. Evol., 38: 3022-3027.
23. Taechowisan, T., W. Puckdee and W.S. Phutdhawong, 2019. *Streptomyces zerumbet*, a novel species from *Zingiber zerumbet* (L.) Smith and isolation of its bioactive compounds. Adv. Microbiol., 9: 194-219.
24. Pfaller, M.A., R.N. Jones, D.H. Walter and Q.C.S. Group, 2001. Proposed quality control guidelines for National Committee for Clinical Laboratory Standards Susceptibility Tests using the veterinary antimicrobial agent tiamulin. Diagn. Microbiol. Infect. Dis., 40: 67-70.
25. van Meerloo, J., G.J.L. Kaspers and J. Cloos, 2011. Cell Sensitivity Assays: The MTT Assay. In: Cancer Cell Culture: Methods and Protocols, Cree, I.A. (Ed.), Humana Press, Totowa, New Jersey, United States, ISBN: 978-1-61779-079-9, pp: 237-245.
26. Pettersen, E.F., T.D. Goddard, C.C. Huang, G.S. Couch, D.M. Greenblatt, E.C. Meng and T.E. Ferrin, 2004. UCSF chimera-A visualization system for exploratory research and analysis. J. Comput. Chem., 25: 1605-1612.
27. Daina, A., O. Michielin and V. Zoete, 2017. SwissADME: A free web tool to evaluate pharmacokinetics, drug-likeness and medicinal chemistry friendliness of small molecules. Sci. Rep., Vol. 7. 10.1038/srep42717.
28. Lamie, P.F. and J.N. Philoppes, 2021. Design, synthesis, stereochemical determination, molecular docking study, *in silico* pre-ADMET prediction and anti-proliferative activities of indole-pyrimidine derivatives as Mcl-1 inhibitors. Bioorg. Chem., Vol. 116. 10.1016/j.bioorg.2021.105335.
29. Pires, D.E.V., T.L. Blundell and D.B. Ascher, 2015. pkCSM: Predicting small-molecule pharmacokinetic and toxicity properties using graph-based signatures. J. Med. Chem., 58: 4066-4072.
30. Kumar, S.N., C. Mohandas, J.V. Siji, K.N. Rajasekharan and B. Nambisan, 2012. Identification of antimicrobial compound, diketopiperazines, from a *Bacillus* sp. N strain associated with a rhabditid entomopathogenic nematode against major plant pathogenic fungi. J. Appl. Microbiol., 113: 914-924.
31. Fdhila, F., V. Vázquez, J.L. Sánchez and R. Riguera, 2003. $_{DD}$-Diketopiperazines: Antibiotics active against *Vibrio anguillarum* isolated from marine bacteria associated with cultures of *Pecten maximus*. J. Nat. Prod., 66: 1299-1301.
32. Drożdżyński, P., N. Rutkowska, M. Rodziewicz and O. Marchut-Mikołajczyk, 2024. Bioactive compounds produced by endophytic bacteria and their plant hosts—An insight into the world of chosen herbaceous ruderal plants in Central Europe. Molecules, Vol. 29. 10.3390/molecules29184456.
33. Tsipinana, S., S. Husseiny, K.A. Alayande, M. Raslan, S. Amoo and R. Adeleke, 2023. Contribution of endophytes towards improving plant bioactive metabolites: A rescue option against red-taping of medicinal plants. Front. Plant Sci., Vol. 14. 10.3389/fpls.2023.1248319.
34. Cimmino, A., A. Bejarano, M. Masi, G. Puopolo and A. Evidente, 2021. Isolation of 2,5-diketopiperazines from *Lysobacter capsici* AZ78 with activity against *Rhodococcus fascians*. Nat. Prod. Res., 35: 4969-4977.
35. Guo, Z.K., R. Wang, F.X. Chen, T.M. Liu and M.Q. Yang, 2018. Bioactive aromatic metabolites from the sea urchin-derived actinomycete *Streptomyces spectabilis* strain HDa1. Phytochem. Lett., 25: 132-135.
36. Yang, L., A. Mahal, Y. Liu, H. Li and P. Wu *et al*., 2017. Two new 2,5-diketopiperazines produced by *Streptomyces* sp. SC0581. Phytochem. Lett., 20: 89-92.
37. Taechowisa, T., T. Chuen-Im and W.S. Phutdhawon, 2025. Antibacterial and anticancer properties of diketopiperazines from *Streptomyces antimicrobicus* BN122, an endophyte in *Oryza sativa* var. glutinosa. Pak. J. Biol. Sci., 28: 27-37.

38. Yu, Z., C. Han, B. Yu, J. Zhao and Y. Yan *et al*., 2020. Taxonomic characterization, and secondary metabolite analysis of *Streptomyces triticiradicis* sp. nov.: A novel actinomycete with antifungal activity. Microorganisms, Vol. 8. 10.3390/microorganisms8010077.
39. Chen, C., Y. Ye, R. Wang, Y. Zhang and C. Wu *et al*., 2018. *Streptomyces nigra* sp. nov. is a novel actinobacterium isolated from mangrove soil and exerts a potent antitumor activity *in vitro*. Front. Microbiol., Vol. 9. 10.3389/fmicb.2018.01587.
40. Fang, Q., F. Maglangit, L. Wu, R. Ebel and K. Kyeremeh *et al*., 2020. Signalling and bioactive metabolites from *Streptomyces* sp. RK44. Molecules, Vol. 25. 10.3390/molecules25030460.
41. Nicholson, B., G.K. Lloyd, B.R. Miller, M.A. Palladino, Y. Kiso, Y. Hayashi and S.T.C. Neuteboom, 2006. NPI-2358 is a tubulin-depolymerizing agent: *In-vitro* evidence for activity as a tumor vascular-disrupting agent. Anti-Cancer Drugs, 17: 25-31.
42. Bertelsen, L.B., Y.Y. Shen, T. Nielsen, H. Stødkilde-Jørgensen, G.K. Lloyd, D.W. Siemann and M.R. Horsman, 2011. Vascular effects of plinabulin (NPI-2358) and the influence on tumour response when given alone or combined with radiation. Int. J. Radiat. Biol., 87: 1126-1134.
43. Goher, S.S., W.S. Abdrabo, G.B. Veerakanellore and B. Elgendy, 2024. 2,5-diketopiperazines (DKPs): Promising scaffolds for anticancer agents. Curr. Pharm. Des., 30: 597-623.
44. Wang, Z., 2017. ErbB Receptors and Cancer. In: ErbB Receptor Signaling: Methods and Protocols, Wang, Z. (Ed.), Springer, New York, ISBN-978-1-4939-7219-7, pp: 3-35.
45. Kurniawan, Y.D., F. Hermawan, L.P. Hastuti, L.A. Marlina and T. Ernawati *et al*., 2025. Design and evaluation of 2,5 diketopiperazine EGFR inhibitors using molecular docking and dynamics simulations. ChemistrySelect, Vol. 10. 10.1002/slct.202406054.
46. Liu, Y., Y. Liang, J. Jiang, Q. Qin, L. Wang and X. Liu, 2019. Design, synthesis and biological evaluation of 1,4-dihydroxyanthraquinone derivatives as anticancer agents. Bioorg. Med. Chem. Lett., 29: 1120-1126.
47. Elmaidomy, A.H., H.A. Alhadrami, E. Amin, H.F. Aly and A.M. Othman *et al*., 2020. Anti-inflammatory and antioxidant activities of terpene- and polyphenol-rich *Premna odorata* leaves on alcohol-inflamed female wistar albino rat liver. Molecules, Vol. 25. 10.3390/molecules25143116.
48. Dewanjee, S., T.K. Dua, N. Bhattacharjee, A. Das and M. Gangopadhyay *et al*., 2017. Natural products as alternative choices for P-glycoprotein (P-gp) inhibition. Molecules, Vol. 22. 10.3390/molecules22060871.
49. Claxton, L.D., G. de A. Umbuzeiro and D.M. DeMarini, 2010. The *Salmonella* mutagenicity assay: The stethoscope of genetic toxicology for the 21st century. Environ. Health Perspect., 118: 1515-1522.